energies

MDPI

*Article*

# Resilience of Residential Hydrokinetic Power Systems: A Practical Approach

**Milton Cuenca [1,2], Carlos Cuenca [3,4], Roberto Pico [1] and Leo Gutierrez [4,*]**

[1] Faculty of Engineering Sciences, Quevedo State Technical University, Quevedo 120304, Ecuador; mcuencac@uteq.edu.ec (M.C.); rpico@uteq.edu.ec (R.P.)
[2] Electrical Department, Warsaw University of Technology, 00-661 Warsaw, Poland
[3] Facultad de Ingeniería Mecánica y Ciencias de la Producción, Escuela Superior Politécnica del Litoral, ESPOL, Guayaquil 090112, Ecuador; cacuenca@alumni.usp.br
[4] Facultad del Mar y Medio Ambiente, Universidad Del Pacifico, Guayaquil 090904, Ecuador
* Correspondence: leo.gutierrez@upacifico.edu.ec; Tel.: +32-468358104

**Abstract**

Work on residential hydrokinetic systems has often concentrated on energy yield or cost, while resilience at the household scale has received less systematic attention. In the present paper, resilience is treated as the main organizing principle for the design of small hydrokinetic schemes for riverine communities with weak or absent grid supply. The proposed framework integrates hydraulic resource assessment, resilience-oriented component selection, regionally calibrated Amazonian demand factors, and quantitative energy storage sizing with analytical LOLP validation. The approach is tested on a tributary of the Napo River near Tena, in Napo Province, Ecuador, where measured INAMHI flow data and Amazonian demand factors ($DF = 0.40 - 0.65$) inform the configuration of a floating axial turbine, a 6 kW PMSG, and a 30 kWh LFP battery bank. Within an operating window of 0.9–2.0 m/s, the system delivers 0.58–6.31 kW and approximately 48 h of autonomy for critical loads.

**Keywords:** resilience; hydrokinetic energy; residential micro-grid

## 1. Introduction

The increasing global demand for sustainable and resilient energy solutions has driven the development of technologies capable of enabling distributed generation, particularly in rural areas and locations with limited access to centralized power grids [1,2]. Among available renewable energy technologies, hydrokinetic turbines have attracted attention for their capability to generate electricity directly from the kinetic energy of flowing water, without requiring dams or significant modifications to river systems [1–3].

This characteristic makes them particularly suitable for applications in environments where preserving natural hydrodynamic conditions is necessary. Ibrahim et al. [1] confirm the environmental suitability of free-flow systems, and Bassey [3] characterizes devices generating power without reservoirs.

Beyond their relatively low environmental impact, these systems can support decentralized energy supply at the household level. When incorporated into residential microgrids, hydrokinetic devices may contribute to improving supply continuity and reducing dependence on a single energy source. However, their effective implementation depends not only on energy conversion efficiency but also on the consideration of

Check for updates

Academic Editor: Massimo Dentice d'Accadia

Received: 27 April 2026
Revised: 21 June 2026
Accepted: 23 June 2026
Published: 28 June 2026

**Copyright:** © 2026 by the authors. Licensee MDPI, Basel, Switzerland. This article is an open access article distributed under the terms and conditions of the Creative Commons Attribution (CC BY) license.

technical constraints, economic feasibility, and local operational conditions that influence long-term performance.

In this context, the present work analyzes the integration of a hydrokinetic energy system for residential use, with emphasis on the behavior of the associated electrical subsystem. The following section outlines the basic principles of energy conversion, providing the basis for the subsequent technical discussion.

Hydrokinetic turbines operate by converting the kinetic energy of water currents into mechanical energy, which is subsequently transformed into electricity. This approach enables the use of flowing water as a renewable energy source, particularly in remote or difficult-to-access areas. Unlike conventional hydropower systems, these devices can operate without large-scale infrastructure, such as reservoirs, which reduces their impact on river morphology and surrounding ecosystems [1–3].

In the design of hydrokinetic turbines, it is necessary to consider the main components involved in the energy conversion process. The blades, or vanes, interact with the water flow and serve as the primary element for energy capture. Their design typically relies on hydrodynamic profiles, such as NACA sections, which Mat Yazik et al. [4] review extensively as the preferred profiles to balance lift generation and drag reduction under expected operating conditions.

The structural response of the blades must also be evaluated by estimating the forces and moments acting on them, which define key parameters such as geometry and angle of attack. In this context, numerical tools are commonly employed, including computational fluid dynamics (CFD) for flow analysis and structural models to assess mechanical behavior. These approaches can be coupled through fluid–structure interaction (FSI) frameworks to obtain a more representative description of turbine performance. Experimental validation is then required to contrast numerical predictions with measured data [5].

The rotor, which supports the blades and transfers the extracted energy into rotational motion, must be designed considering both mechanical integrity and operational conditions. To match the rotational speed of the turbine with the requirements of the electrical generator, a transmission system based on shafts and gears is typically incorporated. A design practice that Puertas-Frías et al. [2] emphasize must account for efficiency and durability, particularly under variable operating conditions commonly observed in riverine environments [2].

The use of hydrokinetic turbines has been proposed as a promising technology within the area of renewable energy for the generation of electric power in urban areas. Palanichamy et al. [6] document a 5 kW microgrid deployment in a secluded Indian community, Jasso-Ruiz et al. [7] demonstrate real-time co-simulation and grid integration of PMSG-based systems, Pompeu et al. [8] develop an electromechanical test bench for energy conversion studies, and Kirke [9] evaluates small axial-flow turbines for remote communities. These systems convert the kinetic energy of moving water in rivers to produce electricity, which has become attractive for hard-to-reach communities.

More of these types of clean energy systems are being developed, and efforts are underway to make them more efficient and reliable [10,11]. This growth is also reflected in recent reports describing multiple field deployments of hydrokinetic power systems, indicating increasing operational maturity beyond laboratory prototypes [12].

The electrical subsystem of a hydrokinetic energy system comprises several interconnected elements [13], including the generator, power electronic converters, energy storage units, and control modules, whose interdependencies are analyzed by Almeida et al. [14] with respect to grid-connected marine hydrokinetic farms. The performance of these components influences the overall efficiency of the energy conversion process, particularly under variable operating conditions [15]. In addition, Jasso-Ruiz et al. [7] demonstrate

PMSG-based hydrokinetic real-time co-simulation and grid integration, confirming the technical viability of the conversion chain.

From an operational perspective, the electrical system must accommodate fluctuations in water flow, ensure adequate power quality, and enable stable integration with local loads or distribution networks. Requirements that Wellinghoff et al. [16] address through regulatory innovation for hydro-kinetic energy development and that Cajot et al. [17] contextualize within multicriteria decision frameworks for urban energy planning. In addition, its design should consider factors such as energy conversion efficiency, load management, and supply continuity to meet typical household energy requirements [18].

The scope covers different aspects of electric power systems for domestic hydrokinetic turbines. The focus is placed on generator technologies and their selection criteria, power electronics including AC–DC–AC converters and grid-tie inverters, control systems for maximum power point tracking (MPPT), and grid synchronization. On this last point, Hu et al. [19] review multi-objective optimization approaches applicable to the organic Rankine cycle, but whose principles extend to hydrokinetic conditioning stages, while Carrasco et al. [20] survey power-electronic systems for grid integration of renewable sources, providing the foundational reference for the converter topologies considered here.

The objectives of this paper are four: (i) to review and evaluate generator technologies, power electronics topologies, and storage under a unified resilience criterion; (ii) to develop a demand characterization methodology using regionally calibrated Amazonian demand factors; (iii) to apply the framework to a Napo River case study with quantitative results; and (iv) to identify regulatory gaps and future research directions.

The novelty lies in the application of an integration approach for all components across the various stages of the conversion process, that is, from hydropower resources to residential load, which has not been demonstrated in previous research on residential-scale hydrokinetic systems applied to the Ecuadorian Amazon.

Hydrokinetic systems for residential applications are still under development; however, they have been considered as a viable alternative for electricity supply in areas without access to conventional grid infrastructure. Several studies have reported the implementation of small-scale systems capable of supplying energy to individual households or small communities [9,21–23].

For instance, Palanichamy et al. [6] document a 5 kW hydrokinetic microgrid in India; Cuenca et al. [23] report Ecuadorian field implementations. Cahill et al. [12] confirm increasing operational maturity through multiple deployments, and Kirke [11] demonstrates that cost-effective residential-scale designs are increasingly viable.

The design of power take-off (PTO) systems has been a relevant aspect in improving the performance of these technologies. Recent developments include compact configurations and transmission mechanisms, such as continuously variable transmissions, aimed at adapting turbine operation to changing flow conditions. In addition, control strategies based on maximum power point tracking (MPPT) have been explored to improve energy extraction under variable operating regimes [24].

Finally, as the field of domestic hydrokinetic energy continues to evolve, addressing challenges related to electric power systems becomes increasingly important [25,26]. The next section details the main components of the electrical power system and their role in ensuring the resilience and efficiency of residential hydrokinetic installations. The analysis, therefore, focuses on evaluating how electrical and control subsystems contribute to the overall resilience and service continuity of residential hydrokinetic microgrids.

## 2. Resilience-Oriented Design Framework

### *2.1. Methodology*

The objective of the proposed methodology is to provide a structured procedure for the preliminary design and evaluation of residential hydrokinetic power systems operating under variable river conditions. The framework integrates hydraulic resource assessment, technology selection, mechanical and electrical sizing, demand characterization, energy storage evaluation, and resilience analysis into a sequential design process.

Unlike conventional approaches that focus on isolated subsystems, the proposed methodology links hydraulic, electrical, and operational aspects to support decision-making during the early stages of project development. The overall methodology is summarized in Figure 1, which presents the proposed resilience-oriented design framework and the interactions between the different stages used to obtain the final system configuration.

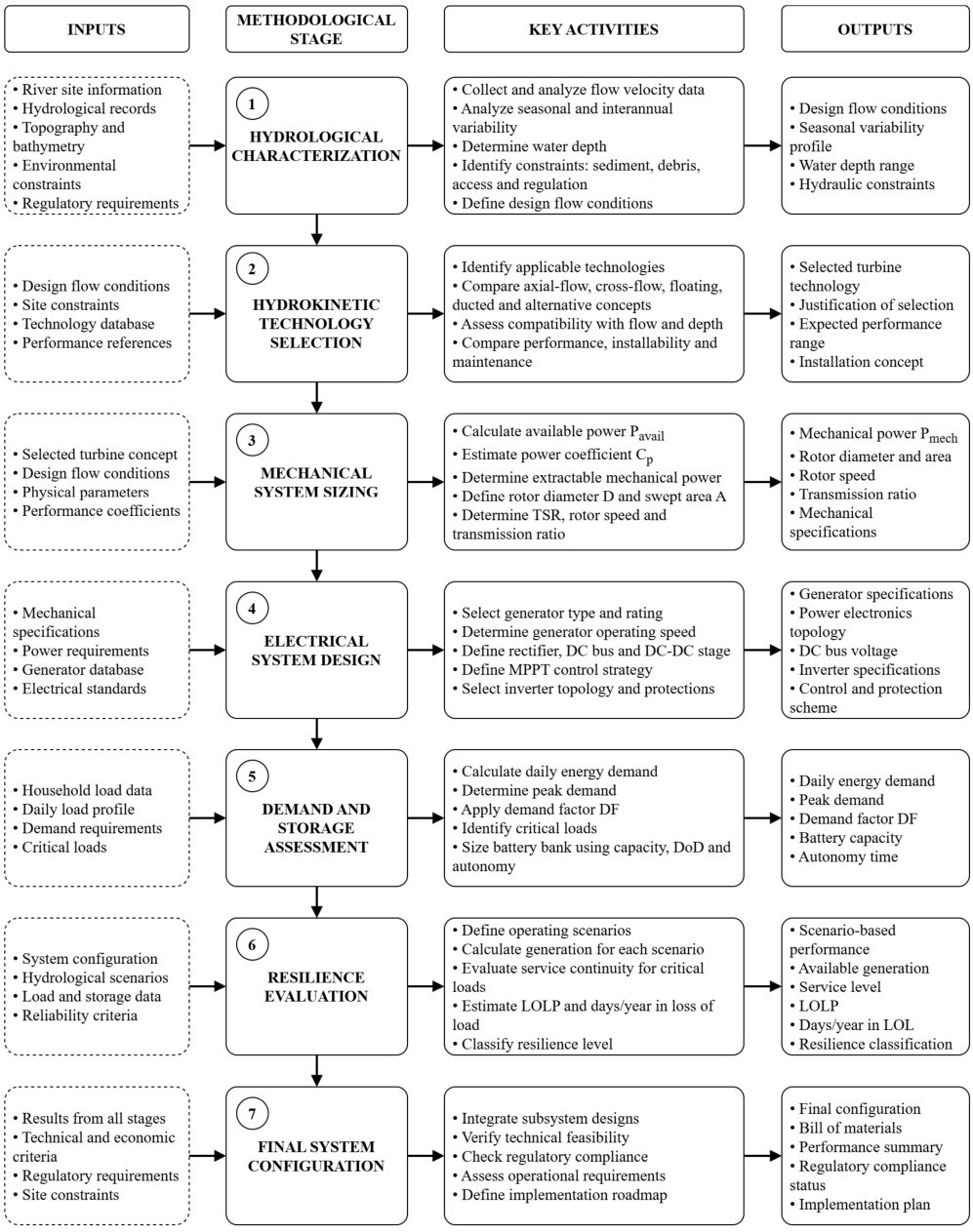



**Figure 1.** Proposed resilience-oriented design framework for residential hydrokinetic power systems.

As illustrated, the proposed framework is organized into seven sequential stages. The process begins with the characterization of the available hydrokinetic resource, followed by the selection of the most suitable conversion technology and the preliminary sizing of the mechanical and electrical subsystems. Subsequently, residential demand and storage requirements are evaluated to establish the operational constraints of the system. Finally, resilience indicators are assessed under different operating scenarios, and the results are integrated into a final system configuration. This structure provides a systematic link between hydraulic conditions, energy conversion, storage capacity, and service continuity requirements for residential hydrokinetic applications.

### *2.2. System Architecture and Standards Compliance*

For hydrokinetic energy systems to work properly, interoperability is essential, i.e., ensuring that electricity generation, conversion, storage, and supply work in harmony as an integrated and resilient whole.

The overall energy conversion chain, from hydraulic energy extraction to electrical power delivery, underpins the system architecture discussed in this section.

It is important to note that compliance with national and international regulations and legislation is a key factor in the design and implementation of these systems. These systems must comply with different safety standards based on the components used, including energy quality, emissions, grid interconnection, and environmental impact. Examples include the updated IEC 60034 standards applicable to generators, IEC 60146 for power electronics, and IEEE 1547 for aspects of distributed resource integration [24–26].

An electrical power system for converting the mechanical energy of a hydrokinetic turbine comprises a set of elements designed to efficiently convert, manage, and distribute the energy produced by the movement of water. Figure 2 shows power system components that are part of the Hydrokinetic turbine system. The modular configuration of these components enhances system resilience by enabling fault isolation and maintaining service continuity under fluctuating hydraulic conditions.

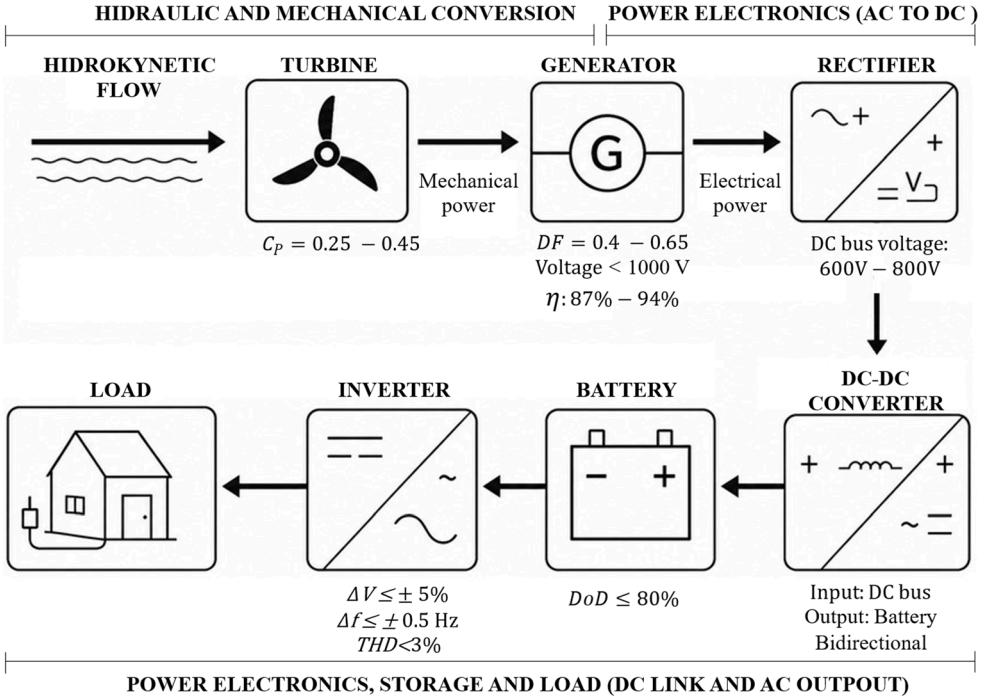



**Figure 2.** Electrical power system components of a residential hydrokinetic turbine and their contribution to system resilience.

The main element is the electrical generator, which can be of the permanent magnet synchronous type (PMSG), which will be responsible for producing electricity [7,27]. This type of generator is chosen because it offers high efficiency, reliability, and capacity to operate at variable speeds, which allows it to perform better under oscillating water flow conditions [28]. This modular architecture enhances system resilience by allowing independent operation of each subsystem, facilitating fault isolation, and enabling continued energy supply under partial component failure or fluctuating hydraulic conditions.

Once the generator has been selected, the power electronics elements are selected, since they will serve in a timely manner to condition and control the electrical output. A key component at this stage is the AC–DC–AC power converter, which typically comprises a rectifier to transform the AC output of the generator to DC, followed by an inverter that produces AC power compatible with the grid [25]. This conversion process enables maximum power point detection (MPPT), which is a control strategy that optimizes turbine power extraction across different water flow rates. Implementing MPPT sometimes means using complex algorithms, such as the "perturb and observe" method, which can improve overall system efficiency [29].

Today, advances in the area of power electronics have enabled the use of wide-bandgap semiconductors, of which silicon carbide (SiC) MOSFETs can be mentioned, for hydrokinetic energy conversion systems [30,31]. These devices offer superior performance in terms of switching speed and efficiency, enabling higher frequency operation and reduced passive component sizes. This is particularly advantageous in subsea applications where space is at a premium.

Batteries should also be considered as part of storage system integration, which is very important in this type of electric power system. The use of this element will allow energy fluctuations to be smoothed out and provide a stable supply during periods of low water flow [29,32]. In more complex designs, pumping systems are incorporated, which will allow reliability and the ability to dispatch energy to the electrical load to be improved.

To connect the power system to the residential area, an inverter must be used, which will allow electricity to be delivered at a frequency and voltage suitable for the operation of the electrical equipment in the homes. In off-grid applications, a microgrid-type design can usually be carried out. Therefore, it should be considered whether it is feasible and necessary to include additional renewable sources, such as creating hybrid systems that will help improve the overall reliability and availability of electrical energy [33].

Finally, control systems must be considered because they are an important part of the electrical power system and manage various aspects, such as energy flow, grid synchronization, and protection against faults. Advanced control schemes, often implemented through digital signal processors or microcontrollers, can significantly improve overall system performance and reliability [34].

Figure 3 shows the flowchart of the requirements to be considered for the selection of the electrical components.

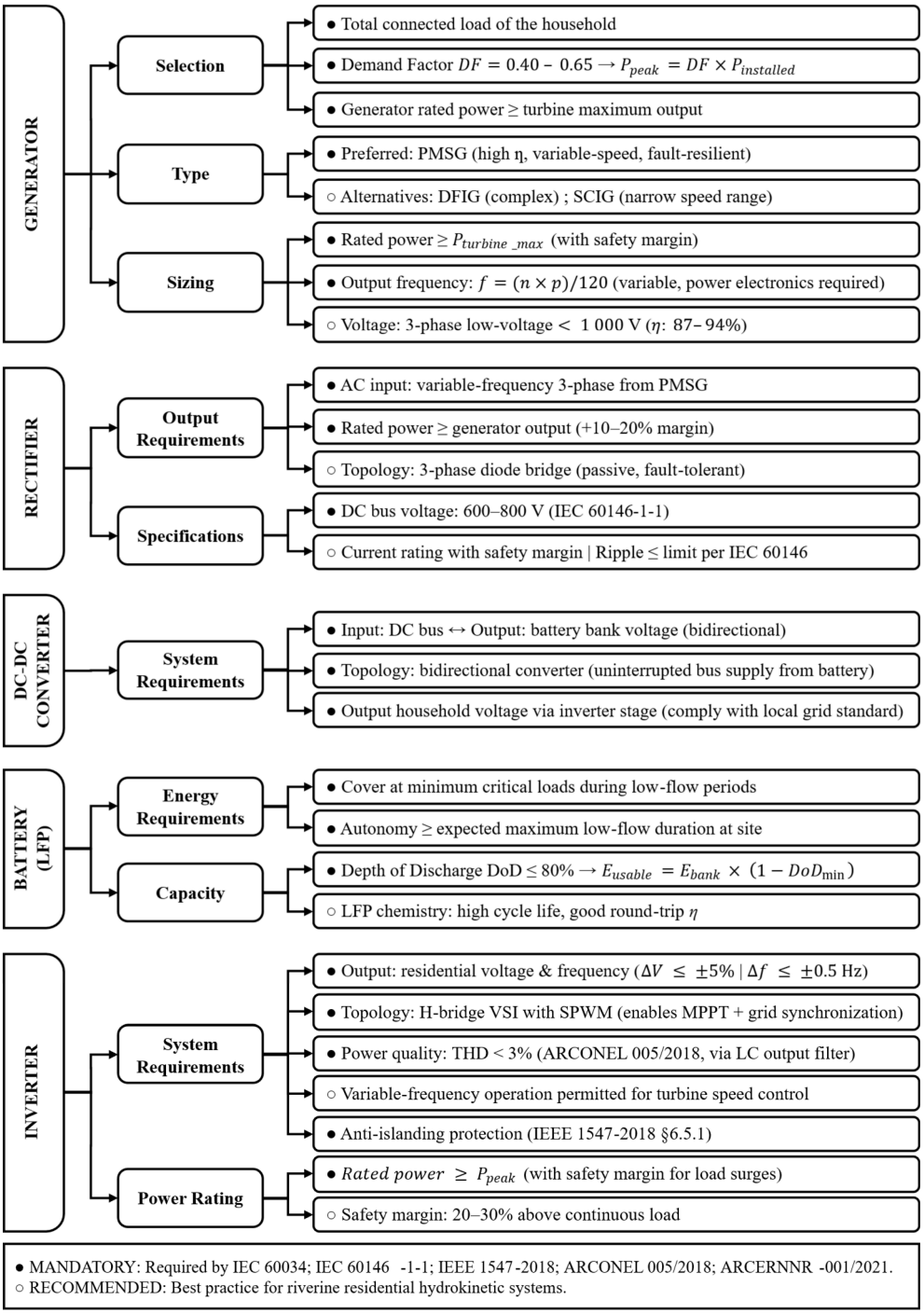



**Figure 3.** Criteria for selecting electrical components in residential hydrokinetic systems with emphasis on reliability and resilience.

## 3. Resilience Aspects

### *3.1. Conceptual Approach to Resilience*

Resilience in distributed power systems refers to the ability of an energy network to anticipate, absorb, adapt, and rapidly recover from disturbances while maintaining acceptable level of performance. Palanichamy et al. [9] demonstrate in their Indian microgrid case study that resilience is linked not only to the continuity of electrical supply but also to the adaptive capacity of both the hydraulic and electrical subsystems under variable flow and load conditions.

Recent studies describe resilience in energy systems as a multi-dimensional property that integrates technical, economic, and operational aspects. It is important to note that reinforcement learning-based multi-energy trading [35] and adaptive energy management under uncertainty [36] are advanced AI-driven strategies that extend the concept of resilience to include smart dispatch and real-time optimization.

From a technical standpoint, it is associated with the reliability of conversion components and the availability of alternative energy paths. The economic dimension relates to the ability of the system to operate within acceptable life-cycle costs, while the operational aspect is linked to its capacity to adapt to variations in flow conditions and changes in electrical demand.

Therefore, assessing resilience in hydrokinetic microgrids requires integrating hydraulic behavior, energy-conversion dynamics, and electrical control performance. These aspects are explored in the following subsections, beginning with the conversion of hydraulic energy into electrical power and continuing with power management, generator selection, and overall system configuration.

### *3.2. Hydraulic-to-Electric Power Conversion*

The conversion of hydraulic energy into electrical power is a key factor determining the resilience and operational efficiency of hydrokinetic systems. The theoretical relationship between flow velocity and generated power follows a cubic dependence, as expressed by:

$$P_{\text{hydraulic}} \propto \rho A V^3 \tag{1}$$

where $\rho$ is the water density (kg/m$^3$), $A$ is the swept area of the turbine (m$^2$), and $V$ is the flow velocity (m/s).

This implies that even modest variations in river velocity can produce significant changes in the available power, underscoring the importance of reliable hydrological assessment. In the literature, low-head and free-flow turbines installed in Latin America typically operate at flow velocities between 0.5 and 3.0 m/s, producing from approximately 100 W to several kilowatts, depending on the turbine diameter, hydrodynamic design, and local flow conditions [32,33].

The estimated energy production was obtained using the standard hydrokinetic power formulation, considering assumed values for the rotor sweep area, power coefficient, and overall system efficiency. Monthly energy estimates were calculated based on average flow velocities and continuous operation over the considered period.

Figure 4 presents the relationship between flow velocity and power for the proposed hydrokinetic system under the conditions of the Napo River Basin. The available hydraulic power, $P_{avail} = \frac{1}{2}\rho A V^3$, is compared with the extracted mechanical power, $P_{extract} = C_p \cdot \frac{1}{2}\rho A V^3$, in order to illustrate the effect of the conversion efficiency within the typical operating range. The calculations were performed using a water density of $\rho = 997 \frac{\text{kg}}{\text{m}^3}$, a rotor sweep area of 4.524 m$^2$ corresponding to a diameter of 2.40 m, and a power coefficient $C_p = 0.35$.

Four operating regions can be identified from the velocity range considered. For velocities below approximately 0.9 m/s, the turbine operates below the cut-in threshold and does not produce useful power. Between 0.9 and 2.0 m/s, which corresponds to typical flow conditions in the Napo River, the estimated power output ranges from approximately 0.58 to 6.31 kW. For velocities between 2.0 and 2.5 m/s, the system may require control strategies, such as pitch adjustment or electrical regulation, to maintain stable operation. At higher velocities, protective mechanisms are required to limit mechanical and electrical loads. The nominal operating point is defined at 2.0 m/s, where the estimated extracted

power is consistent with the nominal capacity of the 6 kW permanent magnet synchronous generator, marked by a short-dashed reference in Figure 4.

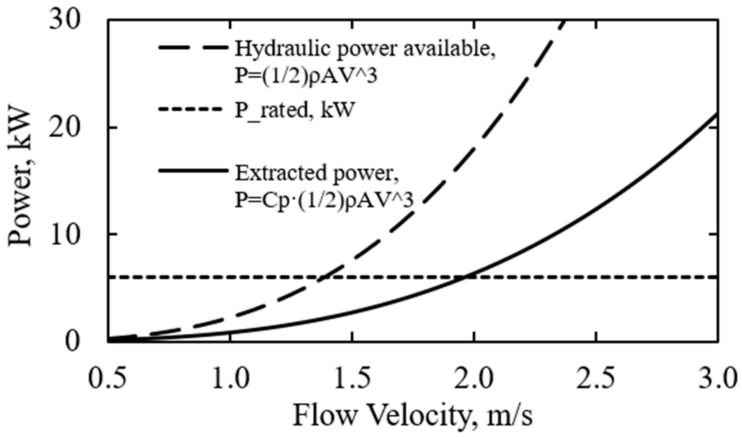



**Figure 4.** Power-Velocity Curve.

A resilience sensitivity annotation highlights that a modest decline in velocity, about 25%, from 1.6 m/s to 1.2 m/s, reduces the extractable power by roughly 58% ($0.75^3 \approx 0.42$), a sensitivity that illustrates how small hydrological variations can markedly affect residential energy availability. This sensitivity directly motivates the storage sizing in Section 4. Hydrological data are specific to a tributary near Tena, Napo Province, and are not generalized to the broader Amazon basin.

### *3.3. Turbine Typologies for Riverine Hydrokinetic Systems*

Hydrokinetic turbines for river and irrigation-channel applications can be classified according to rotor orientation, flow confinement, and installation configuration.

Sood and Singal [34] provide a comprehensive taxonomy of hydrokinetic energy technology across these criteria, Espina-Valdés et al. [37] conduct experimental comparisons between Darrieus and Gorlov turbines under representative riverine conditions, and Niebuhr et al. [38] review hydrokinetic turbines and enhancement techniques for canal installations.

Figure 5 illustrates how the availability of different turbine typologies enables design adaptability, allowing the selection of configurations that balance efficiency, robustness, and maintainability under site-specific hydraulic constraints.

Hydrokinetic turbines can be broadly classified into axial-flow and cross-flow configurations. Axial-flow (horizontal-axis) turbines operate with the rotor aligned with the direction of the current and are typically associated with higher conversion efficiencies, commonly reported in the range of 40–45% for flow velocities above approximately 1.5 m/s. These systems are generally suitable for locations with sufficient depth and relatively stable flow conditions. However, their performance is sensitive to variations in velocity profiles and installation depth, which may limit their applicability in shallow or sediment-laden rivers.

Cross-flow (vertical-axis) turbines, including Darrieus, Savonius, and Gorlov configurations, are characterized by a rotation axis perpendicular to the flow. These systems tend to operate more effectively under turbulent or bidirectional conditions and can be deployed in shallower environments. Their mechanical simplicity can facilitate maintenance and modular implementation. In general, their peak efficiencies are lower than those of axial-flow turbines, typically in the range of 25–35%, and they may be subject to increased structural loading under unsteady flow conditions.

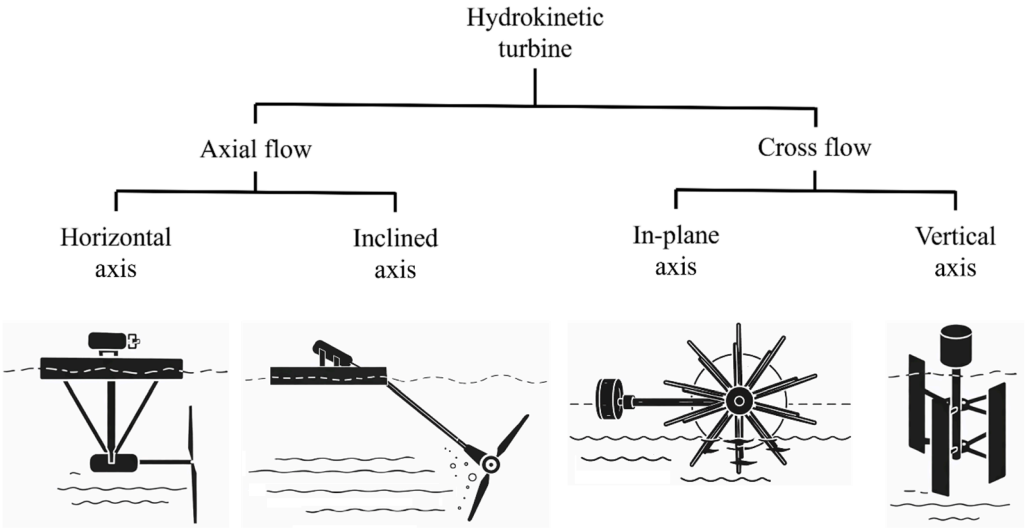



**Figure 5.** Representative configurations of hydrokinetic turbines for river applications. Dashed lines indicate the approximate water free surface.

Ducted or shrouded turbines incorporate flow-guiding structures, such as diffusers, to locally increase the velocity of the water passing through the rotor. This approach can enhance the effective power density, particularly at low natural flow velocities. However, the inclusion of such structures introduces additional complexity in manufacturing and maintenance and may increase sensitivity to debris accumulation.

Floating or surface-mounted configurations have been adopted in rivers with variable depths, where fixed installations are less practical, such as those of the Ecuadorian Amazon. These systems allow relatively rapid deployment and facilitate maintenance operations through easier access and retrieval. Nonetheless, their performance may be affected by stability issues under high-flow conditions or during flood events.

Helical turbines, such as the Gorlov type, represent a variation of vertical-axis designs in which the blades follow a helical geometry. This configuration promotes a more uniform torque distribution and can reduce cyclic loading effects. Despite these advantages, fabrication complexity and associated costs are generally higher than those of simpler configurations such as Savonius turbines [34].

Table 1 summarizes the main characteristics, operating ranges, and applicability of the different turbine configurations for residential-scale hydrokinetic systems. Under flow conditions typical of Ecuadorian rivers, generally characterized by moderate velocities ranging from 0.5 to 2.5 m/s and relatively shallow depths below 2 m, cross-flow and floating axial configurations can be considered suitable options. These configurations offer a compromise among energy conversion efficiency, mechanical robustness, and maintenance requirements, all relevant factors for long-term operation.

Emerging hydrokinetic technologies include oscillatory or hybrid conversion systems that do not rely exclusively on continuous rotational motion. These configurations typically use hydrofoils or blades that undergo controlled oscillatory motion, which is subsequently transformed into rotational energy via mechanical linkages. Such approaches may provide additional flexibility under low or highly variable flow regimes, where conventional turbines tend to operate with reduced efficiency.

These classifications can also be used to define criteria for assessing system performance, including aspects related to reliability, adaptability, and long-term operation under local hydrological conditions.

**Table 1.** Classification of hydrokinetic turbine configurations and their operating conditions for riverine applications [34].

| Turbine Type | Axis Orientation | Typical Velocity Range (m/s) | Main Advantages | Main Limitations |
|---|---|---|---|---|
| Axial-flow | Horizontal | >1.5–3.0 | High efficiency; proven technology | Requires deep, steady flow |
| Cross-flow (Darrieus/Savonius) | Vertical | 0.5–2.0 | Works in shallow/turbulent sites; easy maintenance | Lower efficiency; possible stress under pulsation |
| Ducted/Enclosed | Either | >1.0–3.0 | Increases flow speed; high power density | High cost; clogging risk |
| Floating/Surface-mounted | Various | 0.5–2.5 | Easy installation; adaptable; low civil works | Stability issues in high flow |
| Helical (Gorlov-type) | Vertical | 0.6–2.5 | Smooth torque; fish-friendly design | Moderate cost; complex fabrication |

In the case of Ecuadorian rivers, which are generally characterized by moderate flow velocities and marked seasonal variability, the selection of turbine configuration becomes an important factor in system design. This classification supports the analysis presented in Section 4, where the applicability of small-scale hydrokinetic systems in the Napo River basin is examined. Matching turbine characteristics with local hydraulic conditions can improve operational stability and reduce maintenance requirements, which are relevant considerations for residential energy applications.

### *3.4. Power Considerations*

When designing an electric generation system using a hydrokinetic turbine, one of the most difficult challenges is to improve the overall efficiency of these systems, because it is essential to increase energy production and improve economic viability for domestic use. One of the key aspects is the use of a permanent magnet generator to meet the aforementioned requirements.

Another challenge is the optimization of power electronics components, including maximum power point tracking controllers and more efficient inverters, which can guarantee maximum power extraction from the turbine [39].

One aspect of the mechanical part is the optimal hydrodynamic design that focuses on the turbine blades to reduce resistance, thus increasing efficiency when capturing the energy produced by the movement of water [33].

Due to the variable flow conditions in rivers near residential areas, oscillations in the water flow occur that can affect the consistency and reliability of power generation.

Bassey [3] identifies flow variability as the primary challenge for dam-free hydrokinetic devices, while Arévalo et al. [40] develop a methodology for smoothing power peaks produced by electricity demand and a hydrokinetic turbine for a household load using supercapacitors.

Therefore, solutions must be sought that enable consistent delivery of power to homes.

Integrating these systems with smart grids can help manage variable power outputs by balancing supply and demand and utilizing distributed energy resources. Developing adaptive control algorithms that adjust turbine operating parameters in real time based on flow conditions can improve performance and stability.

In electricity generation and distribution via an optimally designed hydrokinetic turbine for rural homes, selecting system components relies on a set of standardized equations, engineering principles, and compliance with recent regulations.

Generator Selection and Sizing

The selection of generator power cannot be done intuitively, as both the reliability of supply and the economic viability of a residential hydrokinetic system depend on it. In practice, the maximum installed power rarely coincides with the simultaneous use of all household loads, so it is more appropriate to work with the demand factor ($DF$), which allows the effective capacity that the generator must cover under actual operating conditions to be estimated [41–43].

This factor, which helps in properly sizing the generator for real-world loads, is defined as:

$$DF = \frac{Maximum\ Demand}{Total\ Cinnected\ Load} \quad (2)$$

The literature on residential consumption in Latin America has identified demand factors of around 0.65, indicating that peak demand is usually around two-thirds of the total load connected in the home [43–45].

In this context, it should be remembered that, for a household with an aggregate installed load of 10 kW, the expected maximum demand value is around 6.5 kW, which allows the generator to be sized without oversizing and, consequently, to contain investment costs associated with the system.

Figure 6 shows a varied picture of daily residential electricity consumption in the Ecuadorian Amazon, where the demand factor ($DF$) clearly influences the shape of the load curve [46–48]. It is worth noting that in these areas, energy consumption is closely linked to household habits and the tropical climate, which keeps nighttime demand low, around 23–32% of peak load between midnight and the early morning hours. As the population begins its daily activities, a brief spike occurs between 6:00 a.m. and 8:00 a.m. due to the use of induction cooktops and morning household routines. The most pronounced segment occurs at dusk, when the combination of food preparation and artificial lighting raises demand to levels close to the daily maximum, with peaks of 88 to 100%. This pattern repeats, with minor variations, from dispersed rural areas with one to three users per transformer ($DF = 0.40$) to urban centers such as Tena and Puyo ($DF = 0.65$), suggesting a gradual transition that connects the dispersed electrical load of the periphery with the concentration characteristic of urban centers.

It should be noted that, within the electrical demand, the critical loads would be lighting at 0.3 kW, cooling at 0.2 kW, and communications at 0.125 kW, which together total 0.625 kW. Non-critical loads include an electric shower at 4.2 kW, an induction cooktop at 2.0 kW, and fans at 0.5 kW, which may be subject to controlled disconnection in accordance with the priority definition in IEEE 1547.

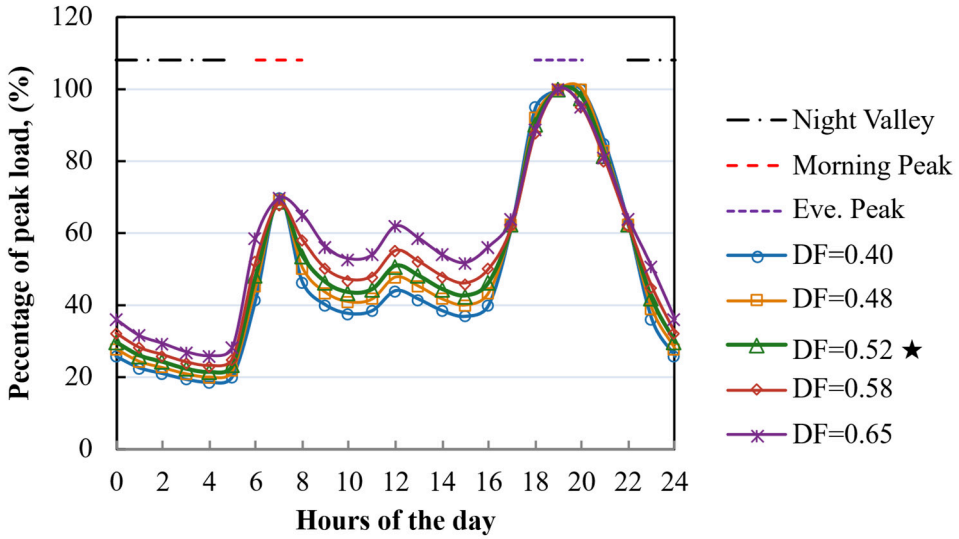



**Figure 6.** Representative daily load curves for residential loads. The star identifies the demand factor ($DF = 0.52$) adopted for the Napo River case study.

### *3.5. Types of Generators for Hydrokinetic Applications*

In a hydrokinetic generation system, it is possible to use different electric machine technologies, including PMSG, doubly fed induction generators (DFIG), squirrel cage induction generators (SCIG), switched reluctance generators (SRG), and synchronous reluctance generators (SynRG). It should be noted that this technological variety opens a range of possible configurations for residential applications, which require careful assessment of the operating characteristics of each generator type before incorporating it into a domestic hydrokinetic system.

A common criterion in the design of hydrokinetic systems is to conduct a comparative study of the performance of each family of generators, so that their advantages and limitations under real operating conditions can be clearly identified. This exercise, which usually incorporates both electrical parameters and operational and maintenance aspects, is particularly useful when the system is intended for residential applications, where the margin for oversizing is limited.

It is worth noting that Figure 7 summarizes this evaluation exercise by comparing the performance of different generators based on indicators such as effective cost, efficiency, simplicity of control schemes, robustness against failures, and the ability to operate at variable speeds, which provides a more solid basis for technological selection in the design of domestic hydrokinetic systems.

Within the set of electrical machines considered for residential hydrokinetic applications, PMSGs tend to occupy a particularly favorable position, as they combine high efficiency with a wide operating speed range, which is especially useful under fluctuating river flow conditions typically found at the household scale [41,49].

This operating flexibility, together with a convenient cost–energy balance over the project lifetime, makes them a suitable option for sites with relatively low flow rates and noticeable seasonal variability, where oversizing other technologies would lead to unnecessary capital expenditure [50].

It should not be overlooked that PMSGs can be configured both in stand-alone schemes and in systems synchronized with the utility grid; in grid-connected arrangements, an appropriate power electronics stage is required to adapt voltage and frequency to residential distribution standards while maintaining adequate power quality and protection functions [39].

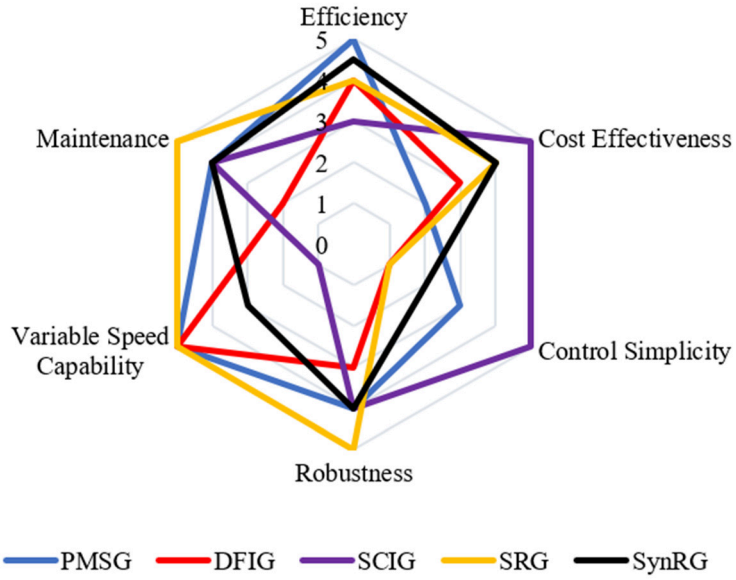



**Figure 7.** Generator performance comparison.

Within the family of induction-based solutions, double-fed induction generators (DFIGs) exhibit a satisfactory response under variable-speed operation, although this advantage is offset by a comparatively high degree of structural and control complexity that limits their overall performance in small residential schemes [51,52].

In contrast, squirrel-cage induction generators (SCIGs) stand out for their low cost and straightforward control requirements, yet their performance deteriorates markedly when they are subjected to broad speed variations, which constrains their suitability for hydrokinetic sites with pronounced flow fluctuations [53].

Within the remaining alternatives, switched reluctance generators (SRGs) emerge as an attractive choice when the design prioritizes mechanical robustness and reduced maintenance needs, since their construction tolerates harsh operating conditions while still delivering acceptable behavior in the other evaluated criteria, with the clear exception of control simplicity, which requires more elaborate electronic and algorithmic implementations [54,55] Synchronous reluctance generators (SynRGs), in contrast, tend to occupy an intermediate position in the comparative assessment, offering moderate performance in efficiency, cost, controllability, and variable-speed capability, without showing a particularly dominant advantage in any single aspect, which situates them as a balanced yet non-specialized alternative for residential hydrokinetic applications [56].

The selection of the operating voltage in residential hydrokinetic systems has a direct impact on system cost, conversion efficiency, and the complexity of integration with existing electrical infrastructure. These aspects are closely related and must be considered simultaneously during the design process.

In practice, the chosen voltage level depends on the specific application requirements, the characteristics of the local grid or load, and the operating limits of the associated power electronic converters.

The comparison of alternative voltage levels for residential hydrokinetic systems highlights the trade-offs that must be considered during the design stage. Single-phase 120/240 V arrangements generally reduce initial investment; however, this benefit is associated with lower power capacity and reduced overall efficiency. In contrast, three-phase 230/400 V configurations provide a more suitable balance for household applications, enabling higher efficiency and improved load distribution without a significant increase in equipment cost. At higher voltage levels, conversion losses tend to decrease and efficiency

improves, although this is accompanied by increased complexity in insulation, protection systems, and power electronics, as well as higher installation and operational costs [57,58].

Table 2 shows the voltage level to be used depending on the different applications in which the hydrokinetic energy system will be used.

**Table 2.** Voltage levels for hydrokinetic systems applications.

| Voltage Level (V) | Application | Generator Types | Power Electronics Required | Grid Connection | Relative Cost | Efficiency (%) |
|---|---|---|---|---|---|---|
| 120/240 | Single-phase residential US | SCIG, PMSG with inverter | Inverter for PMSG | Direct/Transformer | Low | 85–92 |
| 230/400 | Three-phase residential EU | All types | Inverter for PMSG/SRG | Direct | Low | 87–94 |
| 277/480 | Small commercial US | DFIG, SCIG, PMSG | Inverter for PMSG/SRG | Direct/Transformer | Medium | 88–94 |
| 347/600 | Three-phase commercial | DFIG, SCIG, PMSG | Inverter for PMSG/SRG | Transformer | Medium | 90–95 |
| 600 DC | DC microgrid | SRG, PMSG with rectifier | Rectifier only | DC–AC Inverter | High | 90–96 |
| 1000 DC | High voltage DC | SRG, PMSG with rectifier | Rectifier + DC/DC | DC–AC Inverter | High | 88–94 |

Low-voltage configurations are commonly used in small residential hydrokinetic systems, where the expected power demand remains relatively low. Under these conditions, it is possible to employ single-phase generators or three-phase machines adapted to household standards through appropriate transformation stages. This typically results in simpler installation practices, since wiring layouts are similar to conventional residential schemes and equipment interfaces are compatible with standard voltage levels. In addition, electrical clearance requirements are less demanding, which contributes to reducing both design complexity and operational constraints in rural or semi-isolated environments.

For household-scale applications, low-voltage configurations provide a practical balance between technical performance and investment cost, particularly when three-phase systems below 1000 V are considered. These voltage levels allow efficient energy conversion while avoiding the need for specialized insulation or switching devices. They are also compatible with a wide range of generator technologies and generally lead to more compact power electronic stages for energy conditioning and grid interfacing [58].

The selection of the operating frequency is primarily determined by the requirements of the electrical system with which the installation must interact, as well as by the characteristics of the generator. In most cases, standard frequencies are adopted, such as 50 Hz in many regions or 60 Hz in American countries. Variable-frequency operation can also be implemented to provide additional flexibility in turbine speed control, although this approach introduces additional complexity to power electronics and control systems [2].

When variable-frequency operation is used, the turbine can adjust its rotational speed according to the instantaneous flow conditions. This allows a closer correspondence between the available hydraulic resource and the electrical power output. However, this approach requires more advanced power electronic converters and control strategies. It is particularly relevant for generator technologies such as permanent magnet synchronous generators PMSGs and switched reluctance generators SRGs, which are well-suited for variable-speed operation.

### *3.6. Power Electronics Integration*

Power electronics selection significantly impacts system performance, cost, and reliability. The topology choice depends on generator type, voltage levels, and grid connection requirements.

Power-electronics interfacing requirements differ significantly across the generator technologies typically considered for residential hydrokinetic systems, which means that the conditioning stages must be tailored to each machine's electrical behavior and control strategy.

PMSGs usually operate through a rectifier followed by an inverter stage, and in well-designed systems, these links can reach conversion efficiencies on the order of 96%, while double-fed induction generators (DFIGs) tend to rely on back-to-back converters that process only a fraction of the total power and, in doing so, reduce conversion losses compared with full-rating converters. Squirrel cage induction generators (SCIGs) may even be coupled directly to the grid without intermediate power electronics in some configurations, which yields very high overall efficiency, whereas switched reluctance generators (SRGs) demand more sophisticated electronic controllers and modulation schemes but, in return, provide very robust behavior and high tolerance to electrical and mechanical faults, an attribute especially valuable in remote residential hydrokinetic installations exposed to harsh environmental conditions.

Table 3 shows the power-electronics system requirements that must be applied according to the type of generator to be used.

**Table 3.** Power electronic systems according to generator type.

| Generator Type | Rectifier Type | DC Bus Voltage (V) | Inverter Type | Control Complexity | Protection Requirements | Harmonics (THD %) | Power Factor Control | Grid Sync |
|---|---|---|---|---|---|---|---|---|
| PMSG | Diode/PWM | 600–800 | PWM VSI | Medium | Standard | <3 | Yes | Required |
| DFIG | Not required | Not applicable | Back-to-back | High | Advanced | <5 | Yes | Direct |
| SCIG | Not required | Not applicable | Soft starter | Low | Basic | <8 | Limited | Direct |
| SRG | PWM controlled | 600–1000 | PWM VSI | High | Advanced | <5 | Yes | Required |

For the PMSG-based residential system, the following power electronics architecture is specified:

The rectifier is a three-phase diode bridge (passive front-end) with a rated power of 7 kW, providing a 17% margin above the generator's 6 kW output.

The DC bus voltage is 750 V, which strikes a balance between efficiency, insulation requirements in accordance with IEC 60146-1-1, and component availability.

The DC–DC converter will be a bidirectional half-bridge type for a 48 V LFP battery. The MPPT strategy is based on a Perturb & Observe algorithm, with a sampling period selected to be faster than the dominant hydraulic variations expected at the site.

The inverter to be used is a single-phase H-bridge PWM VSI, 110/220 V at 60 Hz with unipolar SPWM modulation.

The recommended filter can be an LC type, where an L = 3 mH and C = 10 μF, which would achieve a harmonic percentage of less than 3% when operating at rated power, thereby complying with ARCONEL Regulation 005/2018.

Regarding the protection system for the aforementioned components, it should be noted that a DC-bus overvoltage crowbar rated at 850 V will be installed, along with an instantaneous-plus-inverse-time AC overcurrent relay, and a passive anti-islanding device using the frequency shift method in accordance with IEEE 1547-2018 §6.5.1.

From a resilience standpoint, in the event of a generator failure, the bidirectional DC–DC converter would allow power to continue being supplied from the battery to the bus, ensuring that critical loads continue to operate continuously. AI-based adaptive power management [35,36] extends this hardware resilience to intelligent dispatch optimization.

## 4. Example of Examination

Ecuador's electricity sector is regulated by the "Ley Orgánica del Servicio Público de Energía Eléctrica (LOSPEE)", a legal framework that explicitly prioritizes renewable sources within the national energy matrix. Under this regulation, a strong dependence on hydroelectric generation has been consolidated, which in 2022 reached around 83.6% of electricity production, an accumulated experience that has historically been associated with large-scale projects, such as the Coca Codo Sinclair plant with an installed capacity of 8640 MW, and which today serves as an institutional benchmark for evaluating new proposals for smaller-scale water-based systems [59].

The Energy Regulation and Control Agency (ARCONEL) is the entity responsible for overseeing the electricity sector in Ecuador, and for establishing the technical and economic conditions under which system operators and users interact. Within this framework, Regulation ARCERNNR-001/2021 includes provisions for distributed generation. However, its implementation has been primarily oriented towards residential photovoltaic systems, which leaves limited regulatory guidance for small-scale hydrokinetic applications. It should not be forgotten that experience in other renewable energy segments shows how certain institutional arrangements and well-articulated policy packages can accelerate the adoption of domestic technologies. This situation invites consideration of whether institutional frameworks of this type could be adapted to residential hydrokinetic projects in remote areas, precisely in a context where the current regulatory vacuum poses both administrative obstacles and a window of opportunity for pioneering initiatives that set precedents for future installations.

The regulatory framework for distributed generation in Ecuador requires compliance with several administrative and technical procedures involving different institutions. ARCONEL requires the registration of distributed generation systems, the verification of equipment specifications, and the establishment of interconnection agreements with local distribution utilities. In addition, Regulation ARCONEL 005/2018 defines power quality requirements that must be met during operation, including voltage deviations within $\pm 5\%$ and frequency variations within $\pm 0.5$ Hz of the nominal values. These limits must be maintained to ensure stable operation and avoid disconnection from the electrical system.

The selected installation site, located on a tributary of the Napo River in the Ecuadorian Amazon region, offers conditions suitable for residential hydrokinetic applications. The area, situated near the city of Tena in Napo Province, at approximately $0^{\circ}50'$ S, $77^{\circ}40'$ W, is characterized by relatively stable flow regimes with moderate seasonal variations of approximately $\pm 25\%$.

This variability is supported by hydrological data collected by the Instituto Nacional de Meteorología e Hidrología (INAMHI), which monitors parameters such as flow velocity, discharge, and water level across the Amazon basin, as illustrated in Figure 8. These observations indicate that river conditions vary over time in response to rainfall patterns and basin-scale processes, which directly affect the kinetic energy available for hydrokinetic conversion.

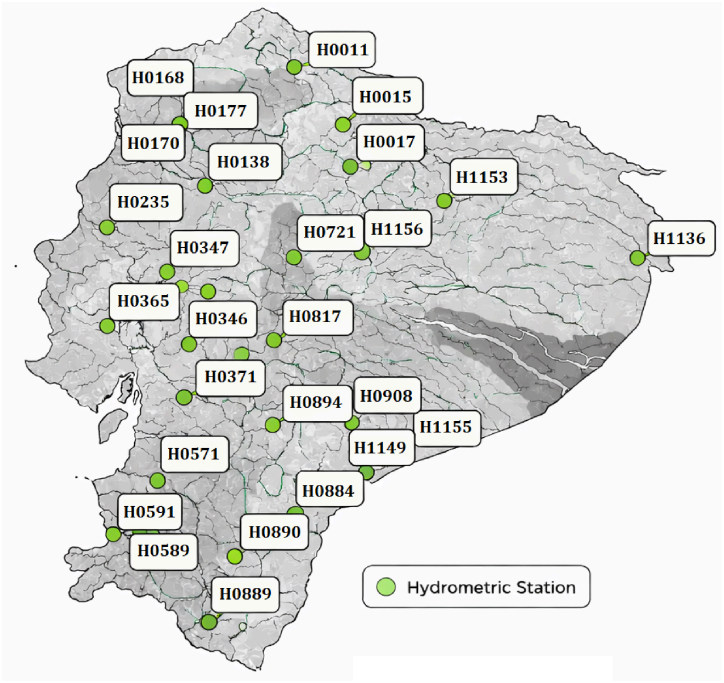



**Figure 8.** INAMHI hydrological monitoring stations in Ecuador.

The integration of these monitoring data enables a more robust characterization of the flow regime in the Napo River basin, reducing uncertainty in the estimation of available energy and supporting more reliable system design.

The catchment area of 450 km$^2$ generates average flow rates of 35 m$^3$/s, maintaining water depths between 3.0 and 4.5 m across the 30-m river width [60].

From an energy perspective, the hydrodynamic conditions of the site have a non-linear effect on power generation, since the extractable power is proportional to the cube of the flow velocity. As a result, relatively small seasonal variations in velocity can lead to noticeable changes in the energy output of the system.

As shown in Figure 9, higher energy production is associated with periods of increased flow, whereas low-flow conditions result in a reduction in generation capacity. This behavior highlights the importance of considering temporal variability during both the design and operation of hydrokinetic systems.

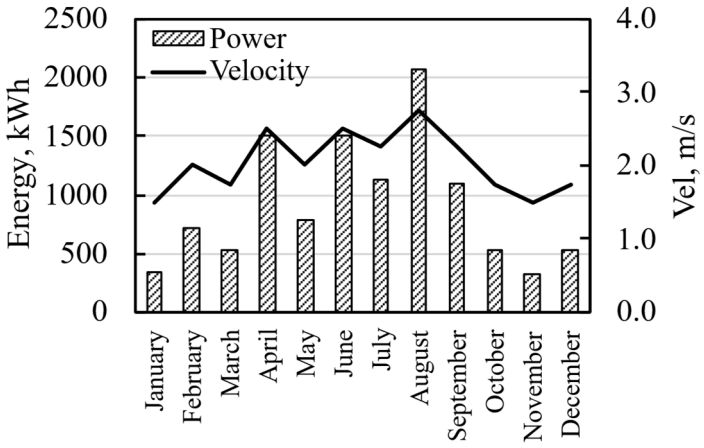



**Figure 9.** Monthly energy production and flow velocity variation for the selected site.

The elevation difference of approximately 520 m provides sufficient gradient for the installation of transmission lines connecting the turbine to the household located about

800 m from the riverbank, enabling the hydrokinetic system to operate in grid-independent island mode. In addition, connection to the regional distribution network operated by EMELNORTE can provide backup supplies during maintenance activities or periods of reduced flow.

The location of the site within indigenous Kichwa territory introduces additional social considerations that must be addressed during project implementation. These include community consultation processes and the establishment of benefit-sharing mechanisms. Rodríguez-Segura et al. [61] demonstrate in their study of social acceptance of renewable energy in southern Spain that perceived fairness, local benefits, and trust between stakeholders influence the long-term acceptance and sustainability of renewable energy projects. For this reason, social aspects should be considered as part of the overall system framework rather than treated solely as external constraints.

The selected residence presents an estimated energy consumption of approximately 13.45 kWh per day, equivalent to about 4900 kWh annually. This level of demand is higher than typical values reported for rural households and is consistent with energy use patterns observed in peri-urban areas of the Ecuadorian Amazon. The load profile reflects local usage conditions, where electric fans are commonly used for cooling instead of air conditioning, and electric showers introduce short-duration peak demands that can reach values close to 4.2 kW.

Based on the site characteristics and the estimated energy demand, the main design parameters considered for the hydrokinetic system are summarized in Table 4.

**Table 4.** Key design parameters for the proposed hydrokinetic system in the Napo River case study.

| Parameter | Value | Justification |
|---|---|---|
| Flow velocity | 1.2–2.0 m/s | Typical Napo River conditions |
| Water depth | 3–4 m | Suitable for floating deployment |
| Installed power | ~6 kW | Matches residential demand |
| Generator type | PMSG | High efficiency at variable speed |
| Gear ratio | 5:1 | Adapts the turbine speed to the generator |

As an illustrative application of the proposed framework, this case study considers representative hydrodynamic conditions in the Napo River basin. Based on the characteristics described in Section 3, the selected site presents mean flow velocities between 1.2 and 2.0 m/s and an average depth of 3–4 m. These conditions are compatible with the operating range of cross-flow and floating axial-flow turbines, which are commonly used under moderate flow regimes due to their relatively simple structure and manageable maintenance requirements. These data are not generalized to the broader Amazon basin.

Seasonal variability has a direct influence on system performance. Flow velocities may exceed 2.5 m/s during high-discharge periods and decrease to values close to 1.5 m/s during low-flow conditions. Given the cubic relationship between velocity and extractable power, these variations can lead to substantial differences in power output, highlighting the sensitivity of hydrokinetic systems to temporal changes in river conditions.

Based on these considerations, a floating axial-flow turbine was selected as a reference configuration. The system is designed to operate at a nominal mechanical output of approximately 6 kW under peak flow conditions. This configuration is consistent with the hydraulic characteristics of the site and facilitates installation, inspection, and maintenance. In addition, it provides a practical basis for the integration of the electrical and control subsystems described in the following sections.

Although this configuration represents a suitable solution for the conditions considered, it does not exclude the use of alternative hydrokinetic concepts. Other conversion

approaches, including non-conventional or hybrid systems, may offer additional flexibility under highly variable flow conditions. Evaluating such alternatives under site-specific scenarios remains an open area of research, particularly in riverine environments such as the Ecuadorian Amazon.

From an operational perspective, the proposed configuration can respond to short-term variations in flow velocity and electrical demand when combined with appropriate power conditioning and storage elements. This capability is relevant in environments where flow conditions are inherently non-steady and may be affected by seasonal variations and debris transport.

Power extraction at the nominal point, that is, by applying the relationship in Equation (1), assuming a velocity of 2 m/s, and using data from the Napo River of $\rho$, $A$, $V$, and a $C_p$ shown in Section 3.2, it is estimated that $P_{extract} = C_p \frac{1}{2} \rho A V^3 = 0.35 \times 0.5 \times 997 \times 4.524 \times 8 =$ 6.31 kW$\approx P_{rated} = 6$ kW.

According to the characterization of demand, a $DF$ of 0.52 can be assumed for the rural part of Napo Province, which is equivalent to a $P_{peak} = 0.52 \times 10$ kW $= 5.2$ kW. Now, assuming the worst-case scenario for an urban area in Tena, where $DF = 0.65$, the peak load would be 6.5 kW. In the second scenario, the 6 kW would be covered by the generator, while the remaining 0.5 kW would be supplied by the battery.

The selected 6 kW permanent magnet synchronous generator is consistent with the estimated mechanical power available from the turbine, while allowing for typical efficiency losses and short-duration overload conditions associated with flow fluctuations. This power rating reflects a compromise between the local hydraulic resource and residential demand, avoiding unnecessary oversizing of the electrical components, which is particularly relevant in decentralized applications.

A 5:1 gear ratio is employed to match the low rotational speed of the turbine with the generator operating range of approximately 350 rpm. For the nominal flow velocity of 2.0 m/s and a rotor diameter of 2.40 m, this ratio gives a turbine speed of about 70 rpm. The resulting tip-speed ratio is approximately 4.4, which is close to the value of 4 commonly recommended for three-bladed hydrokinetic turbines used in electrical generation. Therefore, the selected ratio is considered a reasonable preliminary match between the hydraulic operating point and the generator requirements, although detailed gearbox optimization should be addressed in future design stages.

The generator operates with an efficiency of approximately 94%, which is within the expected range for this power class. In addition, the absence of excitation requirements simplifies the system and reduces auxiliary losses. The IP67 protection rating allows operation under high humidity and occasional exposure to water, conditions that are typical in tropical river environments. The use of a sealed rotor configuration also reduces maintenance requirements and provides sufficient starting torque at low flow velocities.

The power conditioning stage converts the variable-frequency output of the generator into grid-compatible electricity at 220 V and 60 Hz. This process is supported by maximum power point tracking strategies, which adjust the electrical loading according to the instantaneous flow conditions. The rectifier is rated at 7 kW, providing a margin to accommodate transient overloads and reactive power requirements.

The DC bus voltage is set to approximately 750 V, representing a balance between conversion efficiency, insulation requirements, and component availability. The grid-tie inverter operates with an efficiency close to 97.5% within the typical operating range and maintains acceptable power quality levels through appropriate control strategies, including harmonic mitigation and power factor correction.

Energy storage can be incorporated depending on system requirements and operational priorities. A representative configuration includes a lithium iron phosphate battery

system with a capacity of approximately 30 kWh, which allows maintaining essential loads during periods of reduced flow or grid interruptions.

For the storage system, the usable battery energy at 80% depth of discharge (DoD) would be 24 kWh. Considering the critical load of 0.625 kW mentioned in Section Generator Selection and Sizing, this results in an operating time of 38.4 h without any generator support.

The modular 48 V architecture facilitates system expansion and maintenance, although it introduces additional cost and system complexity that must be considered during the design process. A bidirectional DC–DC converter is used to manage power exchange between the battery system and the DC bus.

Therefore, to evaluate the resilience of the proposed system, which operates under conditions different from nominal operating conditions, the possible scenarios shown in Table 5 are analyzed.

**Table 5.** Seasonal resilience scenarios—Napo River tributary, Tena, Ecuador.

| Scenario | Flow Velocity V (m/s) | Extractable Power (kW) | Generation vs. Peak Demand | Critical Loads ($P_{crit}$=0.625 kW) | Resilience Status |
|---|---|---|---|---|---|
| Operating Regime | [m/s] | $C_p = 0.35$, $A = 4.524\ \text{m}^2$ $\rho = 997\ \text{kg/m}^3$ | $DF = 0.52$ $P_{inst} = 10$ kW | Lighting 0.30 kW Refrig. 0.20 kW Comm. 0.125 kW | IEEE 1547-2018 ARCERNNR 001/2021 |
| HIGH FLOW | 2.0 | 6.31 (=$P_{rated}$) | $P_{extract} > P_{peak}$ (+1.11 kW surplus) | ALL supplied Uninterrupted | Full service maintained |
| MEAN FLOW | 1.5 | 2.66 (42% of $P_{rated}$) | $P_{extract} < P_{peak}$ (−2.54 kW deficit) | ALL supplied Uninterrupted | Reduced service |
| LOW FLOW | 1.2 | 1.37 (22% of $P_{rated}$) | $P_{extract} \ll P_{peak}$ (−3.83 kW deficit) | SUSTAINED ~48 h from battery (partial turbine generation) | Critical mode continuity of essential service |

In the case of high flow at a velocity of 2.0 m/s, the resilience status will be "full service maintained" because the extractable power is greater than the peak demand.

On the other hand, if there is an average flow velocity of 1.5 m/s, the generator will operate at a reduced capacity of 2.66 kW, and the battery will be activated with partial discharges, but critical loads will be fully supplied without interruption.

And in the worst-case scenario, where the flow velocity drops sharply to 1.2 m/s, the resilience status indicates "critical mode," meaning power can only be supplied to the home's critical equipment, and therefore the battery is discharged because it will be essential for maintaining service continuity.

As shown in Figure 10, during the first period, when the water velocity is 2.0 m/s, the generator will meet the entire demand, allowing the battery to remain fully charged for the entire 3 days without discharging at any time.

During the second period, when the flow rate is 1.5 m/s, the generated power would not be sufficient to fully cover the afternoon peaks, so the battery discharges during those hours and recharges overnight when demand is low. The daily energy balance is positive, so the SoC recovers each day.

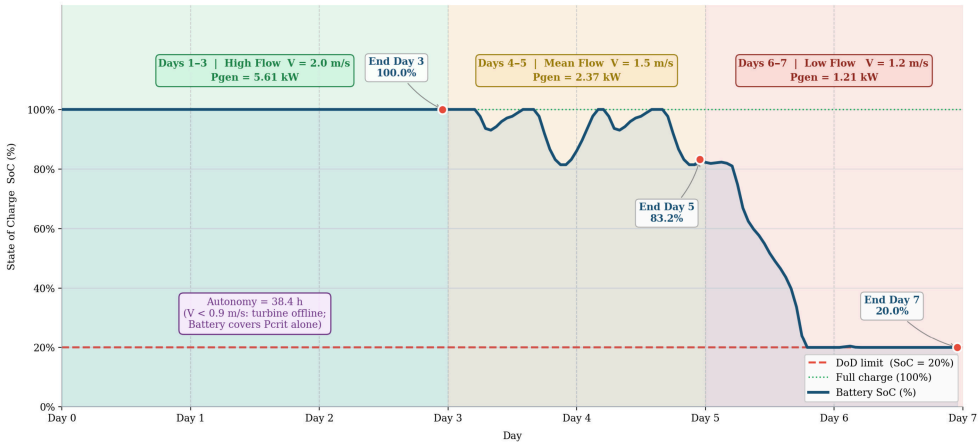



**Figure 10.** Battery SoC Over 7 Day Flow Scenarios.

The third period is considered the most critical because the river's flow rate decreases to 1.2 m/s. During peak demand periods, the battery would be the primary source of power, causing it to discharge significantly and preventing it from recovering energy substantially overnight. Therefore, it is necessary to focus solely on meeting the critical loads of the homes to ensure greater operational autonomy.

Due to the lack of continuous multi-year hourly flow records for this specific tributary, the Loss of Load Probability (LOLP) is estimated to use the Analytical LOLP with a probability distribution of the resource for different scenarios. The daily flow velocity can be modeled as a normal distribution, $V \sim N(\mu, \sigma)$, with different seasonal and operational variations, ranging from 1.2 a 2.0 m/s.

Likewise, a loss of load would occur when $V < V_{cut-in}$, which in this case is 0.9 m/s, causing the battery system's energy to be completely depleted after 38.4 h for critical loads. For the scenario where $\mu = 1.6$ m/s, $\sigma = 0.20$ m/s, the probability of this occurring would be 0.023%, which equates to 0.08 days/year of potential power interruption for critical loads. Table 6 shows several sensitivity analysis scenarios, in which the LOLP remains below 3 days/year even under a conservative scenario.

**Table 6.** Sensitivity Analysis.

| Scenario | $\mu$ (m/s) | $\sigma$ (m/s) | P (V < 0.9) | Days/Year in LOL |
|---|---|---|---|---|
| Optimistic | 1.6 | 0.15 | 0.001% | 0.004 |
| Base | 1.6 | 0.20 | 0.023% | 0.08 |
| Conservative | 1.5 | 0.25 | 0.82% | 3.0 |
| Pessimistic | 1.3 | 0.30 | 4.78% | 17.4 |

Finally, it should be emphasized that the presented configuration represents a conceptual implementation based on typical operating conditions. Actual system performance will depend on site-specific factors such as seasonal discharge, sediment transport, and local hydrodynamic effects. These aspects should be further evaluated through experimental validation and detailed numerical analysis.

## 5. Conclusions

This research demonstrates that residential hydrokinetic power systems can deliver technically sound and operationally resilient energy supply in river-rich regions, provided that component selection, load characterization, and hydraulic variability are addressed through a quantitatively grounded engineering framework.

At the tributary of the Napo River where the case study is set, the hydraulic-to-electric conversion analysis clearly demonstrates the operating range of the system under consideration. A floating axial turbine with a diameter of 2.40 m, a swept area of 4.524 $m^2$, and a power coefficient $C_p = 0.35$ delivers power ranging from 0.58 kW to 6.31 kW when the flow velocity is between 0.9 and 2.0 m/s. It should be noted that the design point is set precisely at V = 2.0 m/s, where the available mechanical power reaches 6.31 kW and aligns consistently with the 6 kW rated power of the selected permanent magnet synchronous generator. The relationship between flow velocity and power generation is highly sensitive due to its cubic dependence. For instance, a reduction in velocity from 1.6 m/s to 1.2 m/s, within the seasonal variation observed in the Napo River basin, leads to a decrease of approximately 58% in extractable power. This behavior highlights the importance of considering energy storage and adaptive control strategies when designing hydrokinetic systems intended to operate under variable flow conditions.

For the household analyzed, the estimated electricity demand is approximately 13.45 kWh per day, corresponding to about 4900 kWh annually. This value is higher than typical rural consumption levels in Ecuador and is consistent with usage patterns observed in peri-urban areas of the Amazon region. When demand factors representative of the province of Napo are considered, with values in the range of 0.40 to 0.65 and a characteristic value close to 0.52, the effective peak demand is reduced to approximately 6.5 kW from an installed capacity of 10 kW. Under these conditions, the selection of a 6 kW permanent magnet synchronous generator is adequate without leading to significant oversizing.

The daily load profile shows a clear peak during the early evening, between 18:00 and 20:00, when demand approaches its maximum value due to the simultaneous use of lighting and cooking appliances. During nighttime hours, typically between midnight and early morning, demand decreases to lower levels, which is consistent with the absence of heating requirements in tropical climates and the concentration of domestic activities during specific periods of the day.

If one looks at the Ecuadorian case with some historical perspective, the central role of hydropower is immediately apparent: in 2022, hydropower accounted for 83.6% of the country's electricity production, reflecting a long history of water-based projects and well-established technical capabilities in this field. It must not be overlooked, however, that this legacy coexists with a regulatory framework for distributed generation that remains heavily skewed toward photovoltaic technology. Regulation ARCERNNR-001/2021 has been applied almost exclusively to residential solar systems and, in practice, leaves small-scale hydrokinetic schemes without an explicit pathway. In areas such as the Napo basin, where the EMELNORTE grid has limited reach and often acts more as a backup than as the primary energy source, this absence of specific rules translates into additional administrative obstacles for community projects. At the same time, it is worth noting that this very absence opens up a regulatory design space that remains largely unexplored for residential hydrokinetic initiatives, which could benefit from the experience accumulated in large hydroelectric power plants but adapted to very different technical and social conditions.

When comparing different types of turbines, the specific conditions of Ecuador's Amazonian tributaries, with flow velocities ranging from 0.5 to 2.5 m/s and depths generally less than 2 m, ultimately tip the balance in favor of floating axial configurations and cross-flow rotors. It should be noted that the former achieve efficiencies of around 40–45% when the velocity exceeds 1.5 m/s, while the latter fall within a somewhat lower range, close to 25–35%, although they offer more stable performance in the face of turbulent currents carrying sediment. It must not be overlooked that, for systems intended

for remote communities, ease of maintenance and the ability to remove the equipment from the riverbed using local resources are just as critical as pure efficiency. From this perspective, channeled or diffuser-based solutions, which can increase the effective flow velocity by around 30–40%, are excluded from the design scheme under consideration, as their construction increases the project's cost and the presence of branches, sand, or suspended debris raises the likelihood of blockages and unscheduled shutdowns that the community itself would struggle to manage.

The numerical results define a consistent range of performance for residential hydrokinetic systems under the conditions considered for the Ecuadorian Amazon. At the selected operating point, the system is able to extract approximately 6.3 kW of mechanical power. The electrical conversion stages operate with efficiencies close to 94% at the generator level and around 97.5% at the inverter stage.

In addition, the inclusion of a 30 kWh battery system allows maintaining critical loads for up to 48 h under complete discharge conditions. Considering a more conservative operating strategy based on an 80% depth of discharge, the available autonomy is approximately 38.4 h, which still provides a significant buffer during prolonged low-flow periods or temporary generation interruptions.

These values are obtained considering a demand factor of approximately 0.52 and seasonal flow variations on the order of $\pm 25\%$. Under these conditions, the system can maintain operation within an acceptable performance range, although the available power remains strongly dependent on flow variability. This behavior is a key aspect when evaluating the operational reliability of hydrokinetic systems in riverine environments.

Sensitivity analysis across four flow scenarios confirms that the LOLP remains below 3 days/year even under conservative assumptions, validating the resilience of the proposed configuration for residential service continuity in the Ecuadorian Amazon.

It should be emphasized that the present study focuses on the development of a resilience-oriented design framework supported by hydrological data, component sizing procedures, regulatory constraints, and representative operational scenarios. Consequently, the results are intended to provide a preliminary engineering assessment of residential hydrokinetic systems rather than a detailed dynamic representation of their electrical behavior. The proposed configuration establishes a consistent basis for future investigations involving coupled electrical simulations, advanced control strategies, and experimental validation under real operating conditions.

Future research should focus on three complementary directions. First, the power–velocity relationship should be experimentally verified under representative operating conditions in the Napo River basin. Second, numerical optimization techniques may be applied to refine blade geometry and improve energy capture within the velocity range of 0.9–2.0 m/s. Finally, detailed electrical simulations incorporating power electronics, battery dynamics, and control strategies should be developed to evaluate system performance under transient operating conditions.

To close, advancing a specific regulatory framework within the ARCERNNR distributed generation framework, without losing sight of the possibility of hybrid couplings with photovoltaic or wind power to cover prolonged periods of low flow.

**Author Contributions:** Conceptualization, M.C.; Methodology, C.C. and L.G.; Software, L.G.; Validation, R.P.; Formal analysis, M.C. and R.P.; Investigation, C.C., R.P. and L.G.; Resources, C.C. and R.P.; Writing—original draft, M.C. and C.C.; Writing—review & editing, R.P. and L.G.; Visualization, L.G.; Supervision, R.P.; Project administration, R.P. All authors have read and agreed to the published version of the manuscript.

**Funding:** This research received no external funding.

**Data Availability Statement:** The original contributions presented in this study are included in the article. Further inquiries can be directed to the corresponding author. reason.

**Acknowledgments:** This article contributes to the results obtained by the Energy Efficiency and Renewable Energies research group of the Electricity program at the Faculty of Engineering Sciences, UTEQ.

**Conflicts of Interest:** The authors declare no conflict of interest.

## Abbreviations

The following abbreviations are used in this manuscript:

| | |
|---|---|
| DF | Demand factor |
| DFIG | Doubly Fed Induction Generator |
| PMSG | Permanent Magnet Synchronous Generator |
| SCIG | Squirrel Cage Induction Generator |
| SRG | Switched Reluctance Generator |
| SynRG | Synchronous Reluctance Generator |
| HVDC | High-Voltage Direct Current |
| LFP | Lithium Iron Phosphate |
| MPPT | Maximum Power Point Tracking |
| NACA | National Advisory Committee for Aeronautics |
| SiC | Silicon Carbide |
| PTO | Power Take-Off |
| THD | Total Harmonic Distortion |
| IEC | International Electrotechnical Commission |
| IEEE | Institute of Electrical and Electronics Engineers |

## References

1. Ibrahim, W.I.; Mohamed, M.R.; Ismail, R.M.T.R.; Leung, P.K.; Xing, W.W.; Shah, A.A. Hydrokinetic energy harnessing technologies: A review. *Energy Rep.* **2021**, *7*, 2021–2042. [CrossRef]
2. Puertas-Frías, C.M.; Willson, C.S.; García-Salaberri, P.A. Design and economic analysis of a hydrokinetic turbine for household applications. *Renew. Energy* **2022**, *199*, 587–598. [CrossRef]
3. Bassey, K.E. Hydrokinetic Energy Devices: Studying Devices That Generate Power from Flowing Water Without Dams. *Eng. Sci. Technol. J.* **2023**, *4*, 1–17. [CrossRef]
4. Yuce y, M.I.; Muratoglu, A. Hydrokinetic energy conversion systems: A technology status review. *Renew. Sustain. Energy Rev.* **2015**, *43*, 72–82. [CrossRef]
5. Anyi y, M.; Kirke, B. Evaluation of small axial flow hydrokinetic turbines for remote communities. *Energy Sustain. Dev.* **2010**, *14*, 110–116. [CrossRef]
6. Mat Yazik, M.H.; Shyang, C.W.; Ishak, M.H.H.; Ismail, F. An overview of blade materials and technologies for hydrokinetic turbine application. *Int. J. Green Energy* **2024**, *21*, 476–499. [CrossRef]
7. Jasso-Ruiz, U.; Rodríguez-Rodríguez, J.R.; Mendoza, E.; Echeverría, C.; Salgado-Herrera, N.M. Real-Time Co-Simulation and Grid Integration of PMSG-Based Hydrokinetic Energy Conversion Systems via Power-Hardware-in-the-Loop Technics. *Energies* **2024**, *17*, 2662. [CrossRef]
8. Pompeu, L.L.; Fonseca, W.S.; Manito, A.R.A.; de Matos, E.O. Protótipo de Bancada Hidrocinética para Estudo Eletromecânico na Conversão de Energia. In Proceedings of the XXIV Congresso Brasileiro de Automática, Fortaleza, Brazil, 16–19 October 2022. [CrossRef] [PubMed]
9. Palanichamy, C.; Wen, T.W.; Naveen, P. A microgrid for the secluded Paana Theertham Kani settlement in India. *Clean Energy* **2022**, *6*, 43–58. [CrossRef]
10. Damayanti, S.; Dinaseviani, A. Mapping of Household Photovoltaic Research in Indonesia: A literature review using bibliometric analysis. *IOP Conf. Ser. Earth Environ. Sci.* **2024**, *1344*, 012014. [CrossRef]
11. Kirke, B. Towards more cost-effective river hydrokinetic turbines. *Energy Sustain. Dev.* **2024**, *78*, 101370. [CrossRef]
12. Cahill, B.; Caspard, M.; Johnson, N.; Davies, S.; Leung y, P. Growing International Operations: Multiple Deployments of Multiple Hydrokinetic Power Systems in 2023. In Proceedings of the Offshore Technology Conference, Houston, TX, USA, 1–4 May 2023. [CrossRef]

13. Zahraee, S.M.; Shiwakoti, N.; Stasinopoulos, P. A Review on Water-Energy-Greenhouse Gas Nexus of the Bioenergy Supply and Production System. *Curr. Sustain. Energy Rep.* **2020**, *7*, 28–39. [CrossRef]
14. Almeida, J.d.S.; Saavedra, O.R.; Oliveira, D.Q. 0Impact of a Grid-connected Marine Hydrokinetic Farm on Distribution Systems. In *2018 IEEE 9th Power, Instrumentation and Measurement Meeting (EPIM)*; IEEE: Piscataway, NJ, USA, 2018; pp. 1–6. [CrossRef]
15. Lopez Mejia, O.D.; Mejia, O.E.; Escorcia, K.M.; Suarez, F.; Laín, S. Comparison of Sliding and Overset Mesh Techniques in the Simulation of a Vertical Axis Turbine for Hydrokinetic Applications. *Processes* **2021**, *9*, 1933. [CrossRef]
16. Wellinghoff, J.B.; Pederson, J.; Morenoff, D.L. Facilitating Hydrokinetic Energy Development through Regulatory Innovation. *Energy Law J.* **2008**, *29*, 397.
17. Cajot, S.; Mirakyan, A.; Koch, A.; Maréchal, F. Multicriteria Decisions in Urban Energy System Planning: A Review. *Front. Energy Res.* **2017**, *5*, 10. [CrossRef]
18. Rivera, M.; Shook, D.; Foust, E. Experimental and Numerical Investigation into Vertical Axis Water Turbine Self-Starting Phenomenon. In Proceedings of the ASME 2020 International Mechanical Engineering Congress and Exposition, Virtual, 16–19 November 2020. [CrossRef]
19. Hu, S.; Yang, Z.; Li, J.; Duan, Y. A Review of Multi-Objective Optimization in Organic Rankine Cycle (ORC) System Design. *Energies* **2021**, *14*, 6492. [CrossRef]
20. Carrasco, J.M.; Franquelo, L.G.; Bialasiewicz, J.T.; Galvan, E.; PortilloGuisado, R.; Prats, M.A.M.; Leon, J.I.; Moreno-Alfonso, N. Power-Electronic Systems for the Grid Integration of Renewable Energy Sources: A Survey. *IEEE Trans. Ind. Electron.* **2006**, *53*, 1002–1016. [CrossRef]
21. Pimentel, H.; McKinney, A.; Henderson, E.; Frankenfield, J.; Beaujean, P.-P.; Dhanak, M. A Power Takeoff Device for a Small Marine Hydrokinetic Turbine Deployed from an Unmanned Floating Platform. In *OCEANS 2023-MTS/IEEE U.S. Gulf Coast*; IEEE: Piscataway, NJ, USA, 2023; pp. 1–6. [CrossRef]
22. Beam, M.J.; Kline, B.L.; Elbing, B.E.; Straka, W.; Fontaine, A.A.; Lawson, M.; Li, Y.; Thresher, R.; Previsic, M. Marine Hydrokinetic Turbine Power-Take-Off Design for Optimal Performance and Low Impact on Cost-of-Energy. In Proceedings of the ASME 2013 32nd International Conference on Ocean, Offshore and Arctic Engineering, Nantes, France, 9–14 June 2013; Volume 8. [CrossRef]
23. Cuenca, C.A.; Barzola, A.S.; Carriel, B.E.; Paredes, R.J. Hydrokinetic turbines, an alternative for the transformation of the Agro-Industrial sector. *E3S Web Conf.* **2024**, *532*, 02003. [CrossRef]
24. *IEEE Std 1547-2018*; IEEE Standard for Interconnection and Interoperability of Distributed Energy Resources with Associated Electric Power Systems Interfaces. Institute of Electrical and Electronics Engineers (IEEE): Piscataway, NJ, USA, 2023.
25. *IEC 60146-1-1:2024*; Semiconductor Converters–General Requirements and Line Commutated Converters–Part 1-1: Specification of Basic Requirements. International Electrotechnical Commission: Geneva, Switzerland, 2024. Available online: https://webstore.iec.ch/en/publication/69109 (accessed on 26 January 2026).
26. *IEC 60034-1:2022*; Rotating Electrical Machines—Part 1: Rating and Performance. International Electrotechnical Commission (IEC): Geneva, Switzerland, 2022. Available online: https://webstore.iec.ch/en/publication/65446 (accessed on 26 January 2026).
27. Bentes, M.H.C.; Lopes, J.J.A.; Pinheiro, K.A.; Custódio Filho, S.D.S.; Vaz, J.R.P.; Mesquita, A.L.A. Torques and Moments of Inertia Models for Horizontal Axis Hydrokinetic Turbine Driveline. *Trends Comput. Appl. Math.* **2023**, *24*, 229–244. [CrossRef]
28. Ileberi, G.R.; Li, P. Integrating Hydrokinetic Energy into Hybrid Renewable Energy System: Optimal Design and Comparative Analysis. *Energies* **2023**, *16*, 3403. [CrossRef]
29. Michas, M.; Ugalde-Loo, C.E.; Ming, W.; Jenkins, N.; Runge, S. Maximum power extraction from a hydrokinetic energy conversion system. *IET Renew. Power Gener.* **2019**, *13*, 1411–1419. [CrossRef]
30. Dai, H.; Acharya, S.; Torrey, D.; Yi, X.; Jasinski, D.; Thomas, R.; Todorovic, M.H.; Rallabandi, V. A Hydrokinetic Energy Conversion System using Underwater LLC-type Resonant Converter. In *2023 IEEE Energy Conversion Congress and Exposition (ECCE)*; IEEE: Piscataway, NJ, USA, 2023; pp. 3273–3278. [CrossRef]
31. Kilgore, T.; Tariquzzaman, M.; Cao, Y. Thermal Management of SiC MOSFETs within Hydrokinetic Applications. In *2022 IEEE Energy Conversion Congress and Exposition (ECCE)*; IEEE: Piscataway, NJ, USA, 2022; pp. 1–8. [CrossRef]
32. Müller, G.; Kauppert, K. Performance characteristics of water wheels. *J. Hydraul. Res.* **2004**, *42*, 451–460. [CrossRef]
33. Diaz Quezada, M.B. Desarrollo de un Prototipo de Turbina Hidrocinética Para la Extracción de Energía en Canales de Ríos y Sistemas de Riego. 2024. Available online: https://www.dspace.espol.edu.ec/handle/123456789/62883 (accessed on 28 January 2026).
34. Sood y, M.; Singal, S.K. Development of hydrokinetic energy technology: A review. *Int. J. Energy Res.* **2019**, *43*, 5552–5571. [CrossRef]
35. Zhang, N.; Yan, J.; Hu, C.; Sun, Q.; Yang, L.; Gao, D.W.; Guerrero, J.M.; Li, Y. Price-Matching-Based Regional Energy Market with Hierarchical Reinforcement Learning Algorithm. *IEEE Trans. Ind. Inf.* **2024**, *20*, 11103–11114. [CrossRef]
36. Li, P.; Cao, Y. A Post-Fault MPPT Control with Multi-Physics Evaluation Framework for Fault-Tolerant Hydrokinetic Turbine Drivetrain. *IEEE Trans. Ind. Appl.* **2026**, *62*, 4378–4391. [CrossRef]
37. Espina-Valdés, R.; Gharib-Yosry, A.; Ferraiuolo, R.; Fernández-Jiménez, A.; Fernández-Pacheco, V.M. Experimental Comparison between Hydrokinetic Turbines: Darrieus vs. Gorlov. *Environ. Sci. Proc.* **2022**, *21*, 26. [CrossRef]

38. Niebuhr, C.M.; van Dijk, M.; Neary, V.S.; Bhagwan, J.N. A review of hydrokinetic turbines and enhancement techniques for canal installations: Technology, applicability and potential. *Renew. Sustain. Energy Rev.* **2019**, *113*, 109240. [CrossRef]
39. Lin, Y.-C.; Balas, V.E.; Yang, J.-F.; Chang, Y.-H. Adaptive Takagi–Sugeno Fuzzy Model Predictive Control for Permanent Magnet Synchronous Generator-Based Hydrokinetic Turbine Systems. *Energies* **2020**, *13*, 5296. [CrossRef]
40. Arévalo, P.; Tostado-Véliz, M.; Jurado, F. A New Methodology for Smoothing Power Peaks Produced by Electricity Demand and a Hydrokinetic Turbine for a Household Load on Grid Using Supercapacitors. *World Electr. Veh. J.* **2021**, *12*, 235. [CrossRef]
41. Kazem, H.A.; Khatib, T. A Novel Numerical Algorithm for Optimal Sizing of a Photovoltaic/Wind/Diesel Generator/Battery Microgrid Using Loss of Load Probability Index. *Int. J. Photoenergy* **2013**, *2013*, 718596. [CrossRef]
42. Pillai, K.; Sundaram, S. Optimization and Feasibility Analysis of Hybrid Distributed Generator Based System with a Comparison of Battery and Hydrogen Energy Storage for Residential Electrification. *Energy Storage* **2024**, *6*, e70075. [CrossRef]
43. Tukkee, A.S.; bin Abdul Wahab, N.I.; binti Mailah, N.F.; Bin Hassan, M.K. Optimal performance of stand-alone hybrid microgrid systems based on integrated techno-economic-environmental energy management strategy using the grey wolf optimizer. *PLoS ONE* **2024**, *19*, e0298094. [CrossRef] [PubMed]
44. Toledo-Cortés, S.; Lara, J.S.; Zambrano, A.; González Osorio, F.A.; Garcia, J.R. Characterization of electricity demand based on energy consumption data from Colombia. *Int. J. Electr. Comput. Eng.* **2023**, *13*, 4798. [CrossRef]
45. Angulo-Paniagua, J.; Victor-Gallardo, L.; Alfaro-Corrales, I.; Quirós-Tortós, J. REEDD-CR: Residential electricity end-use demand dataset from Costa Rican households. *Data Brief* **2023**, *46*, 108829. [CrossRef] [PubMed]
46. Gobierno de la República del Ecuador. Regulación Nro. ARCERNNR-008/2023: Marco Normativo de la Generación Distribuida para el Autoabastecimiento de Consumidores Regulados de Energía Eléctrica, 2023. Available online: https://arconel.gob.ec/wp-content/uploads/downloads/2025/05/Regulacion-Nro.-ARCERNNR-008-23-signed1.pdf (accessed on 6 January 2026).
47. CNEL EP. "Plan Estratégico CNEL EP 2021–2025", 2022. Available online: https://www.cnelep.gob.ec/wp-content/uploads/2022/05/PLAN-ESTRATEGICO-CNEL-EP-2021-2025.pdf (accessed on 6 January 2026).
48. Ministry of Energy and Mines. "Plan Maestro de Electricidad 2023–2032", Quito, Ecuador, 2024. Available online: https://www.ambienteyenergia.gob.ec/plan-maestro-de-electricidad/ (accessed on 6 January 2026).
49. Tarimer, I.; Yuzer, E.O. Designing of a Permanent Magnet and Directly Driven Synchronous Generator for Low Speed Turbines. *Elektron. Elektrotech.* **2011**, *112*, 15–18. [CrossRef]
50. Baqaruzi, S.; Afit Miranto, A.; Wahyuda, D. The Effect of Halbach Array Configuration on Permanent-Magnet Synchronous Generator (PMSG) Outer-Runner. *Int. J. Eng. Sci. Inf. Technol.* **2021**, *1*, 16–23. [CrossRef]
51. Abdolrahimi, H.; Khaburi, D.A. Model predictive control of a brushless cascadedoubly-fed induction generator with torque regulation for stand-alone applications. *Heliyon* **2024**, *10*, e40449. [CrossRef] [PubMed]
52. Müller, S.; Deicke, M.; de Doncker, R.W. Doubly Fed Induction Generator Systems for Wind Turbines: A Viable Alternative to Adjust Speed over a Wide Range at Minimal Cost. *IEEE Ind. Appl. Mag.* **2002**, *8*, 26–33. [CrossRef]
53. Mosobi, R.W.; Chichi, T.; Gao, y.S. Power quality analysis of hybrid renewable energy system. *Cogent Eng.* **2015**, *2*, 1005000. [CrossRef]
54. Li, Z.; Wang, X.; Wei, X.; Liu, L.; Gao, M.; Cheng, L.; Liu, M.; Liu, H.; Sun, H. Implementation and analysis of deflection switched reluctance generator for underwater flow generation applications. *J. Eng.* **2022**, *2022*, 847–856. [CrossRef]
55. Touati, Z.; Mahmoud, I.; Araújo, R.E.; Khedher, A. Fuzzy Super-Twisting Sliding Mode Controller for Switched Reluctance Wind Power Generator in Low-Voltage DC Microgrid Applications. *Energies* **2024**, *17*, 1416. [CrossRef]
56. Adjei-Frimpong y, S.; Muteba, M. Performance Analysis of a Synchronous Reluctance Generator with a Slitted-Rotor Core for Off-Grid Wind Power Generation. *Electricity* **2025**, *6*, 2. [CrossRef]
57. Li, P.; Tariquzzaman, M.; Cao y, Y. A Vienna Rectifier based Grid-Connected Powertrain for Hydrokinetic Turbine Systems. In *2025 IEEE Applied Power Electronics Conference and Exposition (APEC)*; IEEE: Piscataway, NJ, USA, 2025; pp. 3036–3041. [CrossRef]
58. Souza Junior, M.E.T.; Freitas, L.C.G. Power Electronics for Modern Sustainable Power Systems: Distributed Generation, Microgrids and Smart Grids—A Review. *Sustainability* **2022**, *14*, 3597. [CrossRef]
59. Icaza-Alvarez, D.; Jurado, F.; Flores, C.; Ortiz, G.R. Ecuadorian electrical system: Current status, renewable energy and projections. *Heliyon* **2023**, *9*, e16010. [CrossRef] [PubMed]
60. Salinas-León, C.D.; Ochoa-Correa, D. Multicriteria analysis for the site selection of hydrokinetic turbines-HKT for renewable energy generation: A case study in Ecuador. *Renew. Energies* **2025**, *3*, 1–14. [CrossRef]
61. Rodríguez-Segura, F.J.; Osorio-Aravena, J.C.; Frolova, M.; Terrados-Cepeda, J.; Muñoz-Cerón, E. Social Acceptance of Renewable Energy Development in Southern Spain: Exploring Tendencies, Locations, Criteria and Situations. *Energy Policy* **2023**, *173*, 113356. [CrossRef]


**Disclaimer/Publisher's Note:** The statements, opinions and data contained in all publications are solely those of the individual author(s) and contributor(s) and not of MDPI and/or the editor(s). MDPI and/or the editor(s) disclaim responsibility for any injury to people or property resulting from any ideas, methods, instructions or products referred to in the content.